Critical light scattering in liquids

G. Flossmann and R. Folk
Institute for Theoretical Physics, University of Linz, A-4040 Linz, Austria

(Received 21 March 2000)

We compare theoretical results for the characteristic frequency of the Rayleigh peak calculated in one-loop order within the field theoretical method of the renormalization group theory with experiments and other theoretical results. Our expressions describe the nonasymptotic crossover in temperature, density, and wave vector. In addition we discuss the frequency dependent shear viscosity evaluated within the same model and compare our theoretical results with recent experiments in microgravity.

PACS number(s): 05.70.Jk, 64.60.Ht, 62.60.+v, 64.70.Fx

I. INTRODUCTION

Dynamical critical phenomena manifest themselves in a singular temperature dependence of hydrodynamic transport coefficients [1]. In pure fluids these transport coefficients are the thermal conductivity and the shear viscosity, both diverging on approach of the critical point. In Ref. [2] the field theoretic renormalization group (RG) theory has been used for a quantitative description of this nonanalytic behavior and attention was given to the crossover to the analytic behavior in the background further away from T_c. The thermal conductivity can be measured in two ways, (i) by measuring the temperature difference when a heat current flows through the liquid (this is an experiment at zero wave vector k), and (ii) by light scattering experiments in the hydrodynamic region, where the wave vector and the temperature dependent correlation length ξ fulfill the relation $k\xi \ll 1$. In the last case the thermal diffusivity D_T is measured which is related to the thermal conductivity κ_T by $D_T = \kappa_T/(\rho C_P)$ so that for a comparison of the two experimental data the specific heat has to be known. For the thermal diffusivity and the shear viscosity however theoretical calculations show that no other static quantity apart from the correlation length has to be known. This makes these two transport coefficients most suitable to check the dynamical renormalization calculation.

In light scattering experiments in liquids the characteristic frequency ω_c, defined as the half width at half height of the central Rayleigh peak, provides useful additional information about the dynamical properties of the system. Far away from the critical point in the hydrodynamic region the characteristic frequency is given by $\omega_c = D_T(T,\rho)k^2$. Approaching the critical point a crossover from the hydrodynamic to the so-called critical region ($k\xi \gg 1$) takes place and finally at (T_c,ρ_c) the characteristic frequency is a function of the wave vector alone. Asymptotically near the critical point (for very small values of k) the power law behavior $\omega_c \sim k^z$ is expected with the dynamical critical exponent $z \approx 3$. Further away, that means for larger wave vector modulus, a crossover to the background behavior with a nonsingular thermal conductivity takes place. This is described by the van Hove theory where the characteristic frequency behaves as $\omega_c \sim k^4$.

It is the aim of this article to calculate the characteristic frequency in the whole (ξ,k)-plane within the nonasymptotic RG theory in order to describe all types of crossover quantitatively. In addition the density dependence of the line width is considered. The nonuniversal background parameters entering the expression for the characteristic frequency are taken from other dynamical experiments, e.g., measurements of the shear viscosity. Recently very precise data became available for xenon from experiments performed in microgravity [3]. This allows also to reconsider the frequency dependence of the shear viscosity within RG theory already discussed in Ref. [4].

The results for pure fluids are also compared with light scattering experiments in polymer solutions and polymer blends. The nonasymptotic behavior in a mixture is not completely described by the critical model for pure fluids [5] but the asymptotics is the same. Therefore agreement should be found as long as the nonuniversal dynamic parameters are near to their fixed point values.

II. DYNAMIC MODEL

The dynamic order parameter correlation function for the gas–liquid transition can be described within the model H [1], which is a special case of the model H' described in detail in Ref. [2], containing dynamic equations for the order parameter ϕ_0 (the entropy density) and the transverse momentum density $\boldsymbol{j}_t$,

$$\frac{\partial \phi_0}{\partial t} = \mathring{\Gamma}\nabla^2 \frac{\delta H}{\delta \phi_0} - \mathring{g}(\boldsymbol{\nabla}\phi_0)\frac{\delta H}{\delta \boldsymbol{j}_l} + \Theta_\phi, \tag{2.1}$$

$$\frac{\partial \boldsymbol{j}_t}{\partial t} = \mathring{\lambda}_t \nabla^2 \frac{\delta H}{\delta \boldsymbol{j}_t} + \mathring{g}\mathcal{T}\left\{(\boldsymbol{\nabla}\phi_0)\frac{\delta H}{\delta \phi_0} - \sum_k \left[j_k \boldsymbol{\nabla}\frac{\delta H}{\delta j_k} - \nabla_k \boldsymbol{j}\frac{\delta H}{\delta j_k}\right]\right\} + \boldsymbol{\Theta}_t, \tag{2.2}$$

with fast fluctuating forces Θ_i and the projector $\mathcal{T}$ to the direction of the transverse momentum density. The Hamiltonian appearing in the dynamic equations is the normal Hamiltonian of a ϕ^4-theory together with the conserved density $\boldsymbol{j}_t$ entering quadratically:

$$H = \int d^d x \left\{ \frac{1}{2}\mathring{\tau}\phi_0^2 + \frac{1}{2}(\boldsymbol{\nabla}\phi_0)^2 + \frac{\mathring{u}}{4!}\phi_0^4 + \frac{1}{2}a_j \boldsymbol{j}_t^2 \right\}. \tag{2.3}$$

 ©2000 The American Physical Society

As described in Ref. [2] the dynamic equations may be transformed into a dynamic functional leading to dynamic vertex functions which can be calculated in perturbation theory. In general the dynamic scattering function is different from a Lorentzian due to fluctuation effects. This prediction of scaling theory has been observed in ferromagnets [6] and even compared with RG calculations [7]. The same scaling arguments as for the ferromagnet also apply for pure fluids although the deviation from a Lorentzian is expected to be smaller [8]. Moreover it turns out that in one-loop order there are no frequency dependent contributions in the one-loop perturbation terms of the order parameter vertex functions [9]. Therefore the shape of the dynamic correlation function is approximated by a Lorentzian and may be written as

$$\chi_{\mathrm{dyn}}(k,\xi,\omega)=2\chi_{\mathrm{st}}\mathrm{Re}[\mathring{\Gamma}^{-1}_{\phi\tilde{\phi}}(k,\xi,\omega)]=\frac{\chi_{\mathrm{st}}(k,\xi)}{\omega_c(k,\xi)}\frac{2}{1+y^2}, \tag{2.4}$$

in one-loop order with $y=\omega/\omega_c$ and the characteristic frequency ω_c, defined as the half width at half height of the Rayleigh peak. The width is given by the vertex function $\Gamma_{\phi\tilde{\phi}}(k,\xi,\omega=0)$ so that the unrenormalized characteristic frequency reads

$$\mathring{\omega}_c(k,\xi)=\mathring{\Gamma}k^2(\xi^{-2}+k^2)\left(1+\frac{\mathring{f}_t^2}{\xi^{d-4}}\times\int d^dp\frac{1}{1+(\mathbf{x}-\mathbf{p})^2}\frac{\sin^2\theta}{p^2}\right), \tag{2.5}$$

with $x=k\xi$, $\Omega=\omega/\mathring{\Gamma}$, and $\mathring{f}_t=\mathring{g}/\sqrt{\mathring{\Gamma}\mathring{\lambda}_t}$ after setting the parameter $\mathring{w}_\phi=\mathring{\Gamma}/a_j\mathring{\lambda}_t$, which is irrelevant under renormalization, to zero. In full analogy to the renormalization of the transport coefficients [2], the pole in the unrenormalized characteristic frequency may be absorbed into Z-factors using field theoretic renormalization group theory. As we get the same Z-factors (and thus the same flow equations for the Onsager coefficient and the mode coupling) as for the transport coefficients we shall skip the details here.

III. CHARACTERISTIC FREQUENCY

A. General expression

After renormalization the characteristic frequency ω_c is finally found to be

$$\omega_c(k,\xi)=\Gamma(l)k^2(\xi^{-2}+k^2)\times\left\{1-\frac{f_t^2(l)}{16}[-5+6x^{-2}\ln(1+x^2)]\right\}, \tag{3.1}$$

in an ϵ-expansion with $\epsilon=4-d$. The temperature dependence enters via the flow equations for the mode coupling and the Onsager coefficient,

$$f_t^2(l)=f_t^{*2}\left[1+\frac{l}{l_0}\left(\frac{f_t^{*2}}{f_0^2}-1\right)\right]^{-1}, \tag{3.2}$$

$$\Gamma(l)=\Gamma_0\left(\frac{f_0^2}{f_t^{*2}}\frac{l_0}{l}\left[1+\frac{l}{l_0}\left(\frac{f_t^{*2}}{f_0^2}-1\right)\right]\right)^{1-x_\eta}, \tag{3.3}$$

with the one-loop fixed point value of the mode coupling $f_t^{*2}=\frac{24}{19}$ and the one-loop value of the exponent $x_\eta=\frac{1}{19}$. The connection between the flow parameter l and the correlation length or the wave vector, respectively, is found from the matching condition

$$(\xi_0^{-1}l)^2=\xi^{-2}+k^2, \tag{3.4}$$

for the Lorentzian approximation where the correlation length may be expressed in terms of the reduced temperature t via $\xi=\xi_0t^\nu$ with $\nu=0.63$ along the critical isochore. As described in Ref. [4] we may use the cubic model to include noncritical values of the reduced density. In Eqs. (3.2)–(3.4) Γ_0 and f_0 are the initial values of the Onsager coefficient and the mode coupling at an arbitrary reduced temperature t_0 along the critical isochore, l_0 is the solution of the matching condition at t_0 and $k=0$, and ξ_0 is the amplitude of the correlation length. Equation (3.4) is the frequency independent matching condition which has been used since the vertex function $\Gamma_{\phi\tilde{\phi}}$, expressing the characteristic frequency in the Lorentzian approximation, is evaluated at zero frequency.

We may rewrite Eq. (3.1) extracting the asymptotic expressions for the Onsager coefficient and the mode coupling,

$$\omega_c(k,x)=\Gamma_{\mathrm{as}}k^z\left(\frac{1+x^2}{x^2}\right)^{1-x_\lambda/2}[c_{\mathrm{na}}(k,x)]^{x_\lambda}f(k,x), \tag{3.5}$$

with $x=k\xi$ and $z=4-x_\lambda$ where the critical exponent x_λ is given by $x_\lambda=1-x_\eta$ and has the one-loop value $x_\lambda=\frac{18}{19}$. The function $f(k,x)$ is defined as

$$f(k,x)=1-\frac{f_t^{*2}}{16c_{na}(k,x)}[-5+6x^{-2}\ln(1+x^2)]. \tag{3.6}$$

The nonasymptotic contributions are collected in

$$c_{\mathrm{na}}(k,x)=\left[1+\frac{k}{k_0}\sqrt{\frac{1+x^2}{x^2}}\right], \tag{3.7}$$

so that the asymptotic region is characterized by $c_{\mathrm{na}}(k,x)=1$. Finally the asymptotic Onsager coefficient Γ_{as} and the crossover wave length k_0 are given by

$$\Gamma_{\mathrm{as}}=\Gamma_0\left(\frac{f_0^2l_0}{f_t^{*2}\xi_0}\right)^{x_\lambda},\quad k_0^{-1}=\left(\frac{f_t^{*2}}{f_0^2}-1\right)\frac{\xi_0}{l_0}. \tag{3.8}$$

The advantage of Eq. (3.5) over Eq. (3.1) is the clear separation of the asymptotic and the nonasymptotic behavior which will make the discussion of the various limits of the characteristic frequency easier. Before we come to that point in the next section we should remark here that it is also possible to evaluate the crossover function in three dimensions [10] instead of performing an ϵ-expansion. The characteristic frequency then reads

$$\omega_c(k,\xi)=\Gamma(l)k^2(\xi^{-2}+k^2)\times\left\{1+f_t^2(l)\left[\frac{2}{3}\sqrt{\frac{1+x^2}{x^2}}\arctan x-\frac{3}{4}\right]\right\}. \tag{3.9}$$

As expressions (3.1) and (3.9) are almost identical after choosing the right initial values for the Onsager coefficient [see Fig. 3 for a comparison of the asymptotic form of expressions (3.1) and (3.9)] and the mode coupling we shall only discuss the ϵ-expansion result (also used for the evaluation of the transport coefficients in Refs. [2,4]) in the following.

B. Various limits of the characteristic frequency

First we should note that Eq. (3.5) yields a finite value for the characteristic frequency in the *hydrodynamic* limit $x\to 0$,

$$\lim_{x\to 0}\omega_c(k,\xi)=\Gamma_{\mathrm{as}}k^2\xi^{-2+x_\lambda}\left[1+\frac{1}{x_0}\right]^{x_\lambda}\left\{1-\frac{f_t^{*2}}{16}\left[1+\frac{1}{x_0}\right]^{-1}\right\}, \tag{3.10}$$

with $x_0=k_0\xi$. Here the coefficient of k^2 is the nonasymptotic expression for the temperature dependent thermal diffusion coefficient $D_T(\xi)$ discussed in Ref. [2,4] so that we can rewrite Eq. (3.10) in the well-known form $\omega_c=D_T(\xi)k^2$ for the hydrodynamic region. Also in the opposite *critical* limit $x\to\infty$ we obtain a finite value for the characteristic frequency,

$$\lim_{x\to\infty}\omega_c(k,\xi)=\omega_c(k)=\Gamma_{\mathrm{as}}k^z\left[1+\frac{k}{k_0}\right]^{x_\lambda}\left\{1+\frac{5f_t^{*2}}{16}\left[1+\frac{k}{k_0}\right]^{-1}\right\}, \tag{3.11}$$

which is the wave vector dependent nonasymptotic expression of the characteristic frequency. Both nonasymptotic expressions allow to discuss the crossover from the *asymptotic* limit $\xi k_0\to\infty$ or $k/k_0\to 0$ to the *background* limit $\xi k_0\to 0$ or $k/k_0\to\infty$, respectively.

In the hydrodynamic case we obtain the limits

$$\lim_{\xi k_0\to\infty}\omega_c(k,\xi)=\Gamma_{\mathrm{as}}k^2\xi^{-2+x_\lambda}\left(1-\frac{f_t^{*2}}{16}\right), \tag{3.12}$$

$$\lim_{\xi k_0\to 0}\omega_c(k,\xi)=\Gamma_0 k^2\xi^{-2}\left(1-\frac{f_0^2}{f_t^{*2}}\right)^{x_\lambda}, \tag{3.13}$$

where we used the expression for k_0 given in Eq. (3.8) for the last limit. In the background limit our expression reaches the van Hove behavior. In the critical region we obtain

$$\lim_{k/k_0\to 0}\omega_c(k)=\Gamma_{\mathrm{as}}k^z\left(1+\frac{5f_t^{*2}}{16}\right), \tag{3.14}$$

$$\lim_{k/k_0\to\infty}\omega_c(k)=\Gamma_0 k^4\left(1-\frac{f_0^2}{f_t^{*2}}\right)^{x_\lambda}, \tag{3.15}$$

where again we reach the van Hove theory for large values of the ratio k/k_0. This means that our results for the characteristic frequency describe the crossover in the correlation length (from ξ^{-2+x_λ} to ξ^{-2}) in the hydrodynamic region characterized by the limit $x\to 0$ as well as the crossover in the wave vector (from k^z to k^4) in the critical region characterized by the limit $x\to\infty$.

We have seen that with our nonasymptotic theory we always reach the van Hove behavior in the nonasymptotic limit for large values of the wave vector or small values or the correlation length, respectively. This is different from the nonasymptotic mode coupling expression of Olchowy [11], where the characteristic frequency is given by

$$\omega_c(k,\xi)=\frac{k_BT}{6\pi\overline{\eta}^B\xi}k^2\frac{3}{4}(1+x^2)^{-1/2}[-y_D+y_\delta(1+x^2)^{1/2}], \tag{3.16}$$

with

$$y_D=\arctan x_D,$$

$$y_\delta=(1+x_D^2)^{-1/2}[-y_D+\arctan(x_D(1+x_D^2)^{-1/2})], \tag{3.17}$$

depending both on the nonuniversal parameter $x_D=q_D\xi$ which is similar to the parameter k_0 appearing in our nonasymptotic theory. Equation (3.16) does not yield the van Hove theory in the nonasymptotic region but instead becomes negative for $x>2x_D$. This region of unphysical negative values of the characteristic frequency is always reached at constant correlation length when the wave vector becomes larger than the nonuniversal parameter q_D. On the other hand the parameter q_D cannot be set to infinity as this limit yields an unphysical divergence in the hydrodynamic limit for $\xi\to 0$ [11].

C. Discussion of the crossover behavior

In the background we always reach the van Hove behavior for the characteristic frequency. This is a general feature of our nonasymptotic theory. The parameter which describes the crossover from the van Hove expression of the characteristic frequency to its asymptotic expression is in fact the value of the mode coupling f_0 which can take on values from zero to the fixed point value f_t^*. Note that this corresponds to a crossover of k_0 from its asymptotic limit $k_0\to\infty$ to its van Hove limit $k_0\to 0$. The van Hove behavior for $f_0=0$,

$$\omega_c^{\mathrm{vH}}(k,x)=\Gamma_0 k^4(1+x^{-2}), \tag{3.18}$$

is different from the background behavior at finite f_0 so that we can define a background van Hove characteristic frequency ω_c^{BvH} as

$$\omega_c^{\mathrm{BvH}}(k,x)=\Gamma_0 k^4\left(1-\frac{f_0^2}{f_t^{*2}}\right)^{x_\lambda}(1+x^{-2}), \tag{3.19}$$

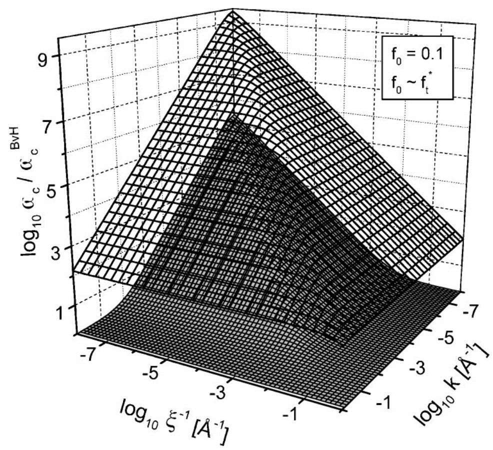

FIG. 1. Ratio of the characteristic frequency ω_c divided by the van Hove background expression ω_c^{BvH} for $f_0=0.1$ or $k_0=7.98\times10^{-3}$ Å^{-1}, respectively (gray surface) where the ratio becomes 1 in the background limit $\xi\rightarrow 0$ and $k\rightarrow\infty$ and for $f_0\approx f_t^*$ (wire frame) where the van Hove expression is never reached by the asymptotic characteristic frequency.

which we now always reach with our nonasymptotic theory in the background limit $\xi k_0\rightarrow 0$ or $k/k_0\rightarrow\infty$, respectively.

Now we can extract the background van Hove behavior from the full characteristic frequency given in Eq. (3.5),

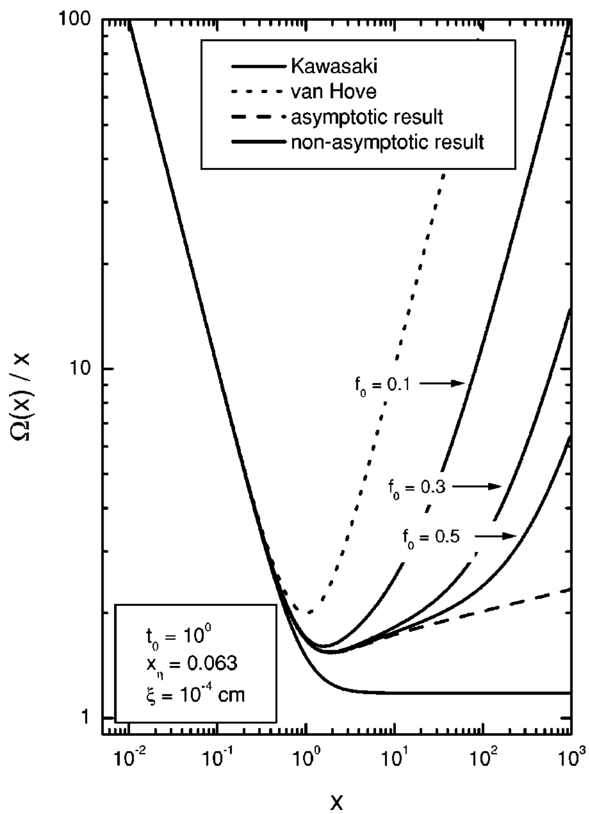

FIG. 2. Comparison of our asymptotic and nonasymptotic (for various values of f_0 at constant correlation length ξ) results for $\Omega(x)/x$ with the Ornstein–Zernike theory and the theoretical result of Kawasaki Ref. [12].

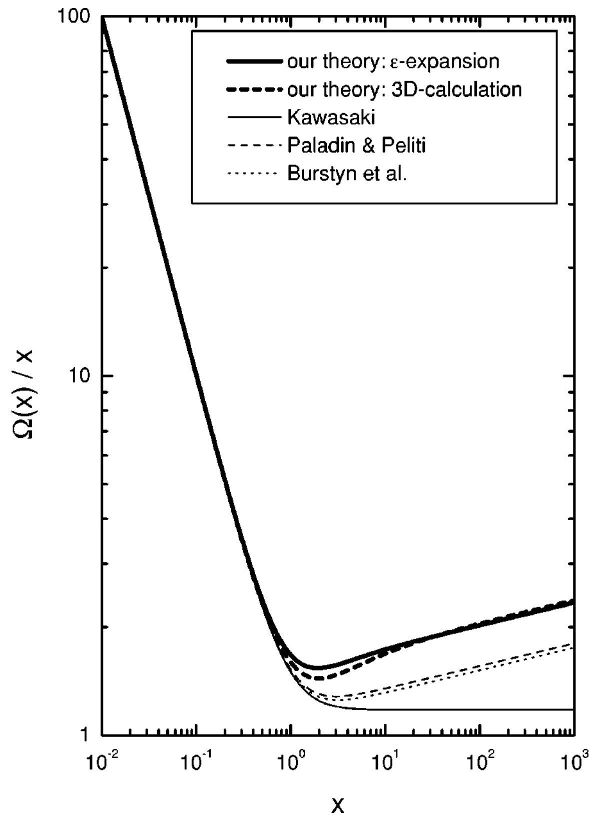

FIG. 3. Comparison of our asymptotic result for $\Omega(x)/x$ evaluated in an ϵ-expansion as well as in three dimensions with the theoretical results of Kawasaki (Ref. [12]), Paladin and Peliti (Ref. [13]), and Burstyn *et al.* (Ref. [14]).

$$\omega_c(k,x)=\omega_c^{\mathrm{BvH}}(k,x)(k\xi_0)^{-x_\lambda}\left(\frac{f_0^2}{f_t^{*2}}l_0\right)^{x_\lambda}\times\left(\frac{1+x^2}{x^2}\right)^{-x_\lambda/2}\left(\frac{c_{\mathrm{na}}(k,x)}{1-\frac{f_0^2}{f_t^{*2}}}\right)^{x_\lambda}f(k,x), \tag{3.20}$$

and plot the ratio $\omega_c/\omega_c^{\mathrm{BvH}}$ in order to demonstrate the crossover behavior of the characteristic line width. This is done in Fig. 1 from which we see that the ratio $\omega_c/\omega_c^{\mathrm{BvH}}$ increases near the critical point (characterized by $\xi\rightarrow\infty$ and $k\rightarrow 0$) as the characteristic frequency then approaches its asymptotic power law behavior, of course with nonuniversal amplitudes depending on value of the mode coupling f_0 in the background. This effect increases with increasing values of the mode coupling f_0. Especially we see that choosing the fixed point value $f_0=f_t^*$ the surface of the characteristic frequency never reaches a flat surface (corresponding to the van Hove behavior).

The crossover from the asymptotic power-law behavior in the critical region, where the characteristic frequency is proportional to k^z, to the van Hove behavior with $\omega_c\propto k^4$ in the nonasymptotic background region can also be seen in Fig. 2 where we compare our asymptotic and nonasymptotic results with the van Hove theory and the result of Kawasaki [12]. To do this we rewrite Eq. (3.5) extracting k^2 instead of k^z,

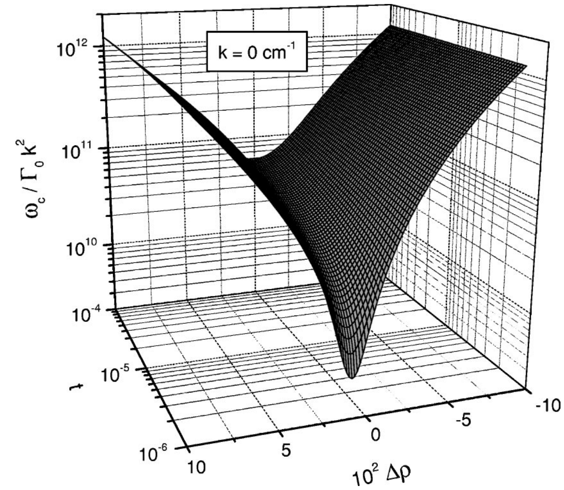

FIG. 4. The characteristic frequency $\omega_c/\Gamma_0 k^2$ as a function of the reduced temperature t and the reduced density $\Delta\rho$ in the hydrodynamic limit for $k=0$.

$$\omega_c^{\rm as}(k,\xi)=\frac{\Gamma_{\rm as}}{\xi^{1+x_\eta}}k^2(1+x^2)^{1-x_\lambda/2}[c_{\rm na}(k,x)]^{x_\lambda}f(k,x)$$

$$\equiv\frac{\Gamma_{\rm as}}{\xi^{1+x_\eta}}k^2\Omega(x), \tag{3.21}$$

and compare the various results for the function $\Omega(x)/x$ at constant correlation length instead of ω_c itself. Therefore we

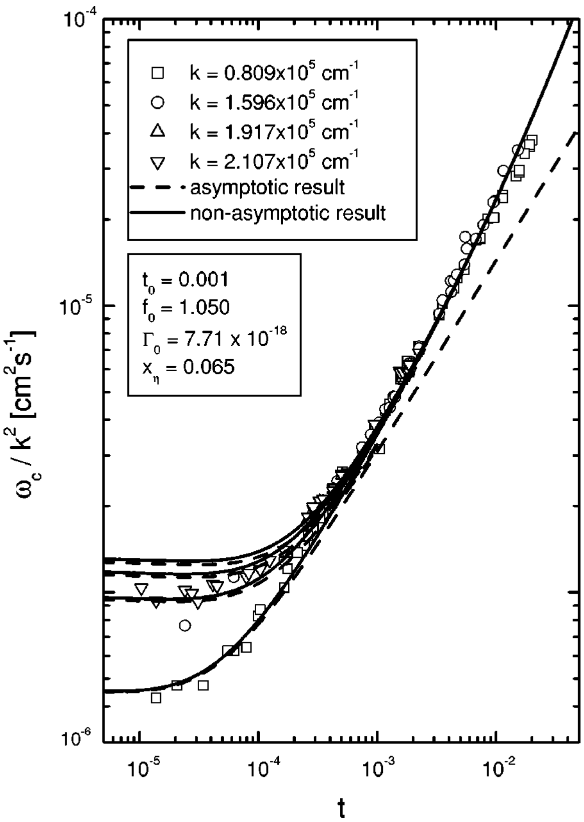

FIG. 5. Comparison of the asymptotic (dashed lines) and nonasymptotic (solid lines) expressions for ω_c/k^2 with the Xe-data of Ref. [16]. The sequence of the curves from top to bottom corresponds to decreasing modulus of the wave vector.

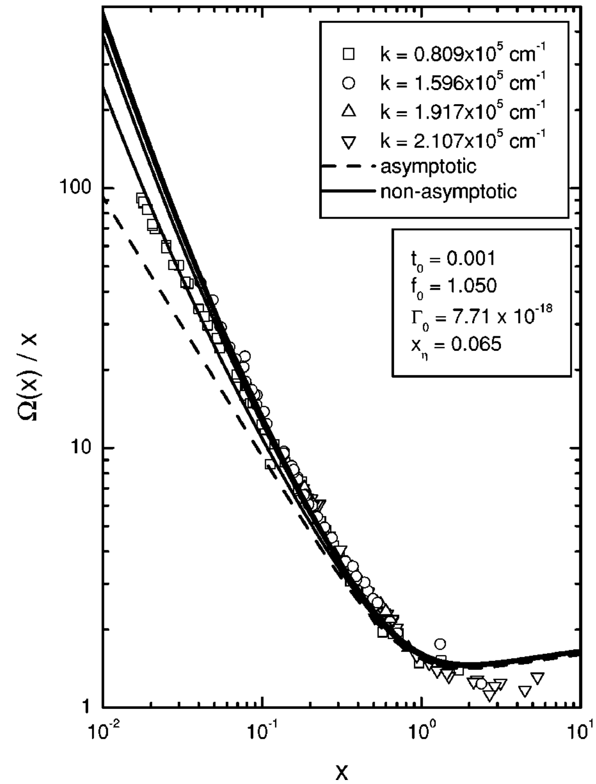

FIG. 6. Comparison of the asymptotic (dashed lines) and nonasymptotic (solid lines) expressions for $\Omega(x)/x$ with the Xe-data of Ref. [16]. The sequence of the nonasymptotic curves from top to bottom corresponds to decreasing modulus of the wave vector.

have to note that the function $\Omega(x)$ defined in Eq. (3.21) is in general not only a function of $x=k\xi$ but also of the wave vector k which enters via the nonasymptotic function $c_{\rm na}(k,x)$. But keeping the correlation length constant as in Fig. 2 we can express k in terms of x so that $\Omega(x)$ is really only a function of x.

As Kawasaki's result is proportional to k^3 instead of k^z the function $\Omega(x)/x$ plotted in Fig. 2 becomes constant for large values of x whereas our asymptotic result (characterized by $c_{\rm na}(k,x)=1$) is proportional to x^{x_η} and the van Hove theory to x. Our nonasymptotic results (at constant values of the correlation length ξ) behave for large values of x like the van Hove theory and are therefore proportional to x. We also see in this figure that the set-in of the crossover to the van Hove theory is determined by initial value of the mode coupling f_0 which is the only free parameter in our nonasymptotic theory. We also should note that in Kawasaki's theory there is a different prefactor for the function $\Omega(x)$ so that we have normalized the function $\Omega(x)/x$ so that the curves coincide for $x\to 0$.

We can also use the function $\Omega(x)$ defined in Eq. (3.21) to compare our asymptotic result for the characteristic frequency with other theories: In Fig. 3 we have plotted the asymptotic result for $\Omega(x)/x$ [which is only a function of x as we have $c_{\rm na}(k,x)=1$] as well as the theoretical results of Kawasaki and Lo [12], Paladin and Peliti [13], and Burstyn *et al.* [14]. As the other authors have a different prefactor for $\Omega(x)$ we have normalized $\Omega(x)$ so that the curves coincide for $x\to 0$. Again we see that the Kawasaki result for $\Omega(x)/x$ becomes constant whereas the other results show the correct

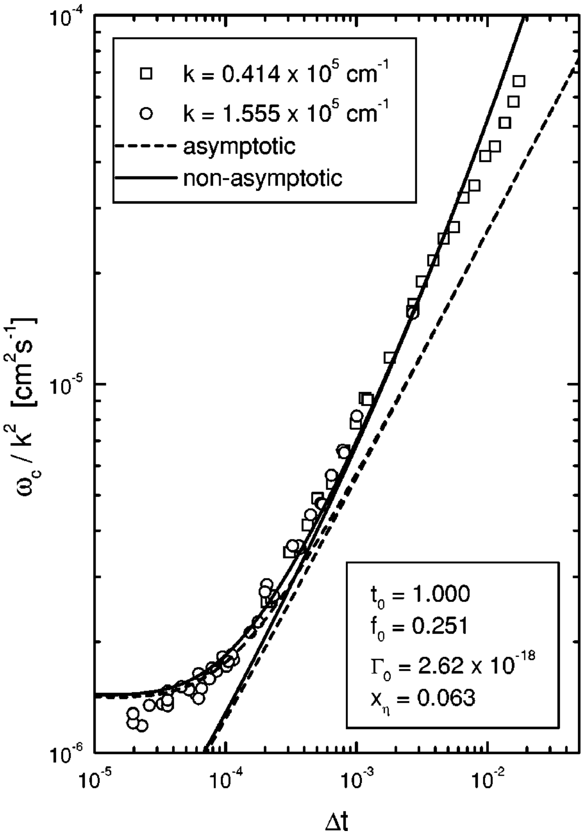

FIG. 7. Comparison of the asymptotic (dashed lines) and nonasymptotic (solid lines) expression for ω_c/k^2 with the CO_2-data of Ref. [16]. The sequence of the curves from top to bottom corresponds to decreasing modulus of the wave vector.

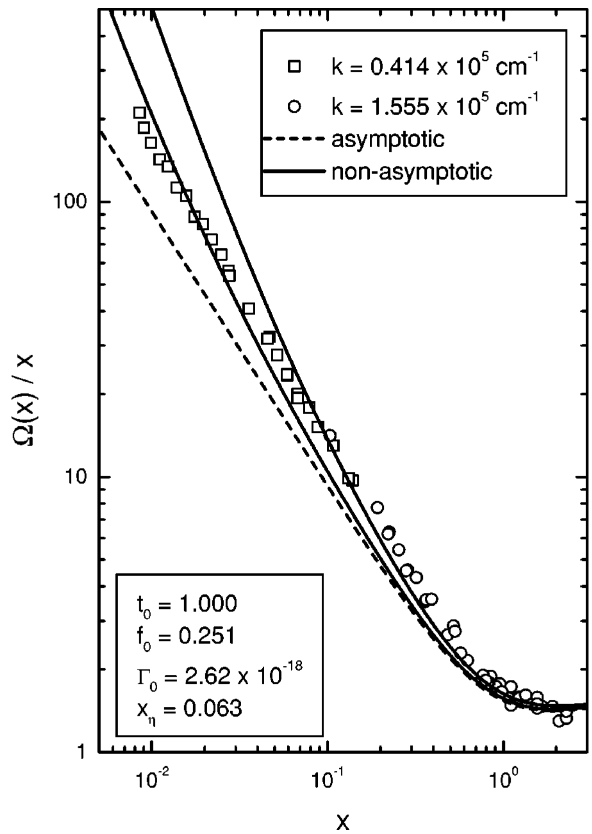

FIG. 8. Comparison of the asymptotic (dashed lines) and nonasymptotic (solid line) expressions for $\Omega(x)/x$ with the CO_2-data of Ref. [16]. The sequence of the nonasymptotic curves from top to bottom corresponds to decreasing modulus of the wave vector.

x^{x_η} behavior for large values of x. An essential difference between our theory and the results of Refs. [12–14] is however that our nonasymptotic theory allows a more apt treatment of background than the purely asymptotic expressions of Refs. [12–14]. In addition to this comparison we should note that at the critical dimension $d=4$ our result for the characteristic frequency is identical with the result of Siggia *et al.* [15].

And finally let us mention that we can extend our theory to noncritical values of the density and calculate the crossover in the characteristic frequency when we leave the critical isochore: Using the parametric representation to connect the correlation length to the reduced temperature $t=(T-T_c)/T_c$ and the reduced density $\Delta\rho=(\rho-\rho_c)/\rho_c$ [4], we are able to evaluate the correlation length as a function of t, $\Delta\rho$, and k. In Fig. 4 we have plotted the characteristic frequency in the hydrodynamic limit for $k=0$ as a function of t and $\Delta\rho$. We see that the characteristic frequency goes to zero in the critical limit $t\rightarrow 0$ and $\Delta\rho\rightarrow 0$ corresponding to $\xi\rightarrow\infty$.

IV. COMPARISON WITH EXPERIMENTS

A. Pure liquids

In Figs. 5–8 we compare our asymptotic and nonasymptotic results for the characteristic frequency ω_c/k^2 as a function of the reduced temperature t and the function $\Omega(x)/x$ as a function of x with experiments in Xe and CO_2 [16] (all nonuniversal parameters are given in Table I). As discussed in Ref. [4] we can treat the exponent $x_\lambda=1-x_\eta$ as an additional free parameter so that we can fit f_0 and x_η from the experimental data (the initial value of the Onsager coefficient Γ_0 is determined by the value of the shear viscosity at t_0). But this means that we need additional data for this fit. In Xe we have used the recent shear viscosity data of Berg *et al.* [3] discussed in the next section. Fitting the parameter f_0 from the characteristic frequency data (the exact value of x_η does hardly affect the exponent $x_\lambda=1-x_\eta$) and the exponent x_η from the shear viscosity data we find good agreement for the characteristic frequency (Figs. 5 and 6) as well as for the frequency dependent shear viscosity (Figs. 11 and 12). For CO_2 we have taken t_0, f_0, and Γ_0 (also given in Table I) from the comparison of the shear viscosity and the thermal diffusivity with experiments in Ref. [4] so that the curves shown in Figs. 7 and 8 are obtained without any free parameter!

As we can see in these figures the experimental data are not described correctly by our asymptotic expressions but only by the nonasymptotic expressions which show the crossover to the van Hove theory for large values of the reduced temperature t or small values of the variable x, respectively. Analogously any asymptotic theory [12–14] fails to describe the experimental data correctly. In Ref. [16] this problem was eliminated adding a regular background contribution of the form $\omega_c^B=(\lambda^B/\rho c_p)k^2(1+x^2)$ to the critical expression for the characteristic frequency with λ^B being the

TABLE I. Nonuniversal parameters of Xe, CO_2, and polydisperse polystyrene (PDPS).

Liquid	ξ_0[Å]	t_0	f_0	Γ_0[cm^4/s]	x_η	ν	k_0[cm^{-1}]
Xe	1.84	0.001	1.050	7.71×10^{-18}	0.065	0.63	48.0×10^5
CO_2	1.60	1.000	0.251	2.62×10^{-18}	0.063	0.63	32.8×10^5
PDPS	4.60	0.100	0.350	2.52×10^{-20}	0.065	0.70	4.66×10^5

regular part of the thermal conductivity and c_p the full specific heat at constant pressure containing also critical contributions. The use of the full specific heat together with the term $1+x^2$ ensures the crossover to the van Hove theory for large values of the reduced temperature as well as for large values of the wave vector (the background characteristic frequency is proportional to $k^2\xi^{-2}$ for $x\to 0$ and to k^4 for $x\to\infty$) so that the full characteristic frequency $\omega_c=\omega_c^C+\omega_c^B$ obtained by this procedure yields basically the same curves as our nonasymptotic theory (see Fig. 6 of Ref. [16]). In our theory however we use a different form of the background characteristic frequency: Following the discussion of the regular background added to the transport coefficients [4] we would have to add a background of the form $\omega^B=D_T^B(T,\rho)k^2-D_T^B(T_c,\rho_c)k^2$ to our results with the background thermal diffusivity given by $D_T^B=\lambda^B/\rho c_p^B$ and the background specific heat c_p^B containing only the regular temperature dependence without the critical singularity. As this background term turns out to be negligibly small in the temperature range shown in Figs. 5–8 we have neglected it so that our asymptotic and nonasymptotic curves for Xe and CO_2 contain only the critical contributions discussed in this article. So the main difference between our nonasymptotic theory and the results of Refs. [12–14] is that the crossover to the van Hove theory, which is clearly seen in experiments, is already contained in our expressions for the characteristic frequency and not added by an appropriate form of the background contribution

In Fig. 6 and 8 we also see that the nonasymptotic results for $\Omega(x)/x$ do of course not collapse on a single curve (in contrary to our asymptotic result and the theories of Refs. [12–14]) as the nonasymptotic contribution $c_{\rm na}$ does not only depend on the variable $x=k\xi$ but also on the wave vector k and the correlation length ξ separately. This behavior can also be seen in the Xe and CO_2 data in Fig. 6 and 8 although the experimental data are not precise enough for a true confirmation of the validity of our nonasymptotic theory.

B. Polymer solutions and blends

And finally we apply our theory for the characteristic frequency to light scattering experiments in binary polymer so-

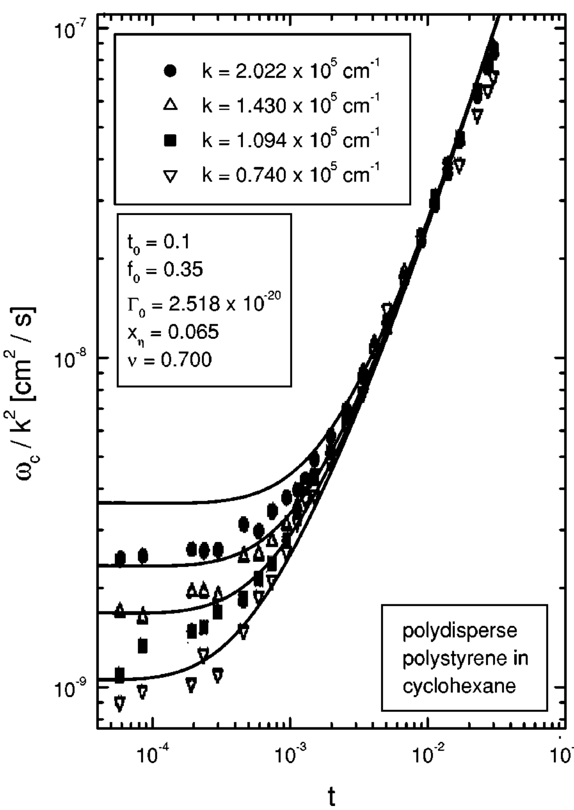

FIG. 9. Comparison of the nonasymptotic characteristic frequency ω_c/k^2 with the experimental data of Ref. [17] in a polymer solution after subtracting the regular background. The sequence of the curves from top to bottom corresponds to decreasing modulus of the wave vector.

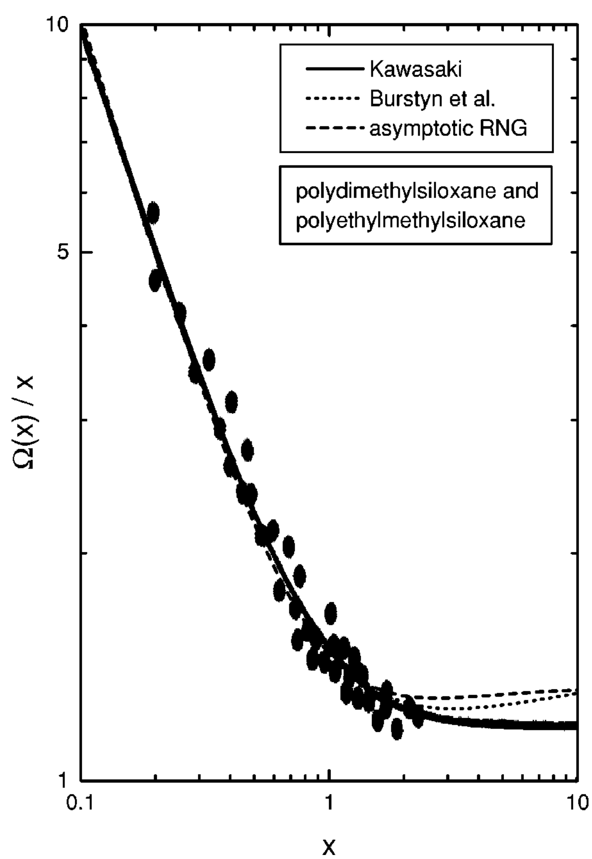

FIG. 10. Comparison of the asymptotic expression for $\Omega(x)/x$ with the experimental data of Ref. [18] in a polymer mixture.

lutions: In Fig. 9 we compare our nonasymptotic theory for the characteristic frequency ω_c/k^2 as a function or the reduced temperature with experimental data in a solution of polydisperse polystyrene (PDPS) in cyclohexane [17]. For this figure the initial value of the Onsager coefficient was determined from the value of the background shear viscosity at the critical point also measured in Ref. [17]. The amplitude of the correlation length ξ_0 as well as the exponents $\nu=0.7$ and $x_\eta=0.065$ were taken from the same article. Therefore we have to note that the exponent ν found by Ref. [17] for the polymer solution is higher than the value $\nu=0.63$ found for pure liquids or liquid mixtures. Fitting the initial value of the mode coupling f_0, which is the only free parameter in our theory, from the experimental data (all values given in Table I) we reach a satisfactory description of the experimental data although the curves for large wave vectors lie above the experimental data for small values of the reduced temperature. Nevertheless we have to note that the quality of the description cannot be compared to the one reached for Xe and CO_2 as there are no detailed experimental data for the shear viscosity of this polymer solution in the vicinity of the critical point available, so that an exact determination of $\overline{\eta}_0$ and thus of Γ_0 was not possible and also the critical exponent had to be fixed and could not be fitted from the experiments.

However one crucial point remains: The fact that we have used the nonasymptotic theory developed for pure liquids to describe a polymer solution is of course a problem as liquids and liquid mixtures do have the same asymptotic behavior but show a slightly different crossover to the nonasymptotic behavior. But as an asymptotic theory is not able to describe the experimental data (in the same way as we were not able to describe the characteristic frequency in pure liquids with the asymptotic theory) and a nonasymptotic theory for critical light scattering in mixtures has not yet been set up, we believe that the systematic errors made by applying a nonasymptotic theory for pure liquids to mixtures (which basically means setting the additional parameter w_3 found for the transport coefficients in liquid mixtures [5] to zero) are rather small and can be tolerated. In addition we have to note that a background characteristic frequency given in Ref. [17] was subtracted from the experimental data as well as from the nonasymptotic results for ω_c/k^2.

In Fig. 10 we compare our asymptotic result for the function $\Omega(x)/x$ as well as the theoretical results of Kawasaki [12] and Burstyn *et al.* [14] with experimental data in the polymer blend of polydimethylsiloxane and polyethylmethylsiloxane [18]. As all these data are only available in a rather small range of x we can apply the asymptotic theory and avoid the discussion of the last paragraph. The use of a nonasymptotic theory would also not be possible for a comparison with these experimental data for a second reason: All data shown in Fig. 10 were obtained for different temperatures and wave vectors but these different values of k and ξ were not indicated separately in the article but only the corresponding value of $x=k\xi$. This was also the reason why we could not fit the initial value of the Onsager coefficient so that the only fit parameter, the prefactor of $\Omega(x)$, was set by the choice that our result shall coincide with the result of Burstyn *et al.* in the limit of small values of x. In addition we have to note that the experimental values for the function $\Omega(x)$ were obtained from the data for the characteristic frequency dividing not by the full shear viscosity depending on the correlation length but only by its constant background value, so that we had to correct this, multiplying our theoretical expression for the function $\Omega(x)$ by x^{-x_η}. In any case the experimental data shown in Fig. 10 are not precise enough to favor any of the presented theoretical expressions.

V. FREQUENCY DEPENDENT SHEAR VISCOSITY

Since we have used information from the shear viscosity in the discussion of the light scattering line width we shall add an analysis of the most recent shear viscosity data for Xe [3] to this article. These new data allow a much more detailed analysis of the frequency dependent shear viscosity leading to slightly different parameters than the discussion of the shear viscosity of Xe in Ref. [2] which was based on older data. In Ref. [4] we have discussed the theoretical expression for the frequency dependent shear viscosity, which is given by

$$\overline{\eta}(t,\Delta\rho,\omega)=\frac{k_BT}{4\pi}\frac{\xi_0}{lf_t^2(l)\Gamma(l)}\times[1+E_t(f_t(l),v(l),w(l))], \tag{5.1}$$

with the one-loop perturbational contribution

$$\begin{aligned}E_t(f_t(l),v(l),w(l))=&-\frac{f_t^2}{96}\Bigg\{1+6\left[i\frac{v^2}{w}\ln v+\frac{1}{v_+-v_-}\left(\frac{v_-^2}{v_+}\ln v_--\frac{v_+^2}{v_-}\ln v_+\right)\right]\\&-\frac{4}{(v_+-v_-)^3}\left[\frac{v_+^3-v_-^3}{3}+\frac{3}{2}(v_+-v_-)(v_+^2\ln v_++v_-^2\ln v_-)-(v_+^3\ln v_+-v_-^3\ln v_-)\right]\\&+\frac{2}{(v_+-v_-)^2}\left[\frac{v_+^3}{v_-}(1+4\ln v_+)+\frac{v_-^3}{v_+}(1+4\ln v_-)\right.\\&\left.+\left(\frac{1}{v_-}-\frac{2}{v_+-v_-}\right)\frac{v_+^4\ln v_+-v^4\ln v}{v_-}+\left(\frac{1}{v_+}+\frac{2}{v_+-v_-}\right)\frac{v_-^4\ln v_--v^4\ln v}{v_+}\right]\Bigg\}.\end{aligned} \tag{5.2}$$

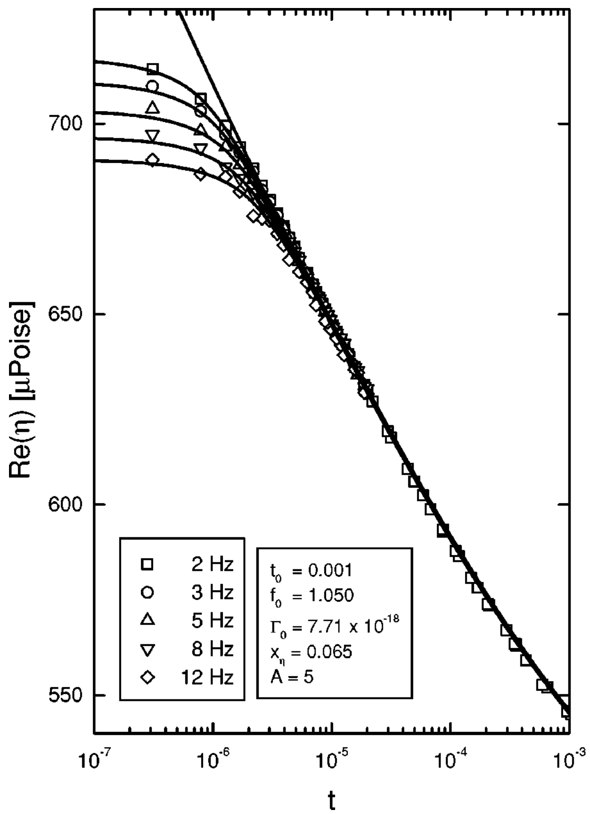

FIG. 11. Comparison of the theoretical expression for the real part of the shear viscosity in microgravity at various frequencies with the experimental data of Ref. [3]. See text for details.

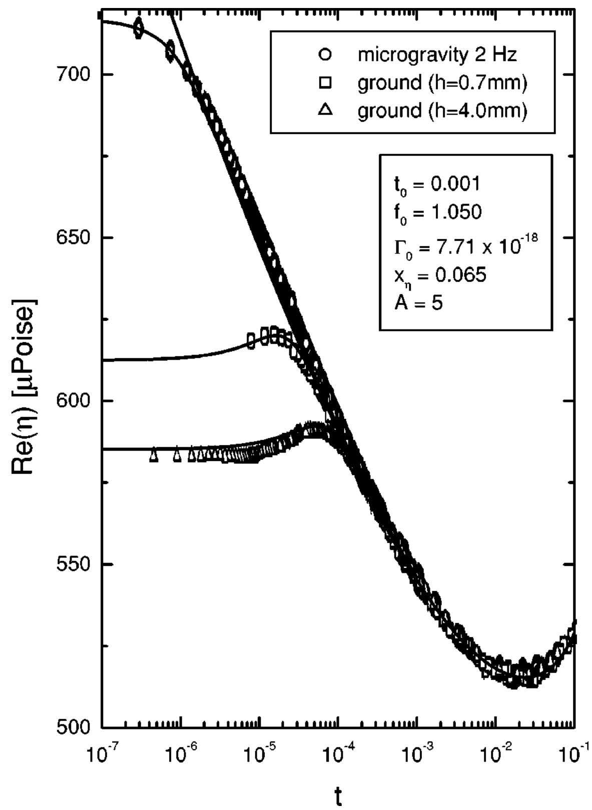

FIG. 12. Comparison of the theoretical expressions for the real part of the shear viscosity in microgravity (at frequencies 0 and 2 Hz) as well as in earthbound experiments (for two different vessel heights) with the experimental data of Refs. [3,21].

The parameters introduced in Eq. (5.2) are defined as

$$v(l)=\frac{\xi^{-2}(t)}{(\xi_0^{-1}l)^2}, \quad w(l,\omega)=\frac{\omega}{2\Gamma(l)(\xi_0^{-1}l)^4}, \tag{5.3}$$

$$v_{\pm}(l,\omega)=\frac{v}{2}\pm\sqrt{\left(\frac{v}{2}\right)^2+iw}, \tag{5.4}$$

with the mode coupling $f_t(l)$ and the Onsager coefficient $\Gamma(l)$ given by Eqs. (3.2) and (3.3). The mode coupling parameter l is now a function of the correlation length ξ and the frequency ω and results from the solution of the matching condition [19]

$$\left(\frac{\xi_0}{\xi}\right)^8+\left(\frac{2\omega}{\Gamma(l)}\right)^2=l^8. \tag{5.5}$$

At the moment of publication no experimental data were available to compare them to our theoretical expressions. The situation has changed meanwhile as Berg *et al.* [3] performed shear viscosity experiments at small frequencies in a microgravity environment onboard a space shuttle. Comparing their experimental results with the mode coupling theory [20], they found that they could only describe their data correctly multiplying the frequency by a factor of 2 in the theoretical expressions. They explained the introduction of this factor as a two-loop effect correcting the errors of the one-loop expression used for the frequency dependent shear viscosity. With this multiplicative factor for the frequency they were able to reproduce the experimental data for the shear viscosity very well.

In Figs. 11 and 12 we compare our theory with experimental data in microgravity and in the earth's gravitational field [3,21] fitting the exponent x_η with f_0 taken from the light scattering experiments of Ref. [16]. In doing so we found $x_\eta=0.065$ instead of the value $x_\eta=0.069$ used by Berg *et al.* We should note here that we can use the exponent $x_\eta=0.069$ (with the initial values $f_0=0.959$ and $\Gamma_0=8.82\times10^{-18}$ cm^4/s) to get exactly the same theoretical curves as shown in Figs. 11 and 12 but then we are not able to describe the characteristic frequency data correctly with this choice of f_0 and Γ_0. This fact that the parameters f_0 and x_η cannot be determined unambiguously from the shear viscosity data alone was already discussed in detail in Ref. [4].

In Figs. 11 and 12 it turns out that we can describe the experimental data in microgravity only if we multiply the frequency by a factor of 5, which may be explained as corrections to the one-loop expressions from higher order perturbation contributions [22] and thus justified for the same reason as the factor of 2 in the mode coupling theory [3]. But then we are able to describe not only the microgravity data but also the earth-bound experiments very well with a single set of parameters shown in Table I. And once again let us mention that we have used the same set of parameters to describe the characteristic frequency in Xe correctly in Figs. 5 and 6. As the experimental data shown in Fig. 12 cover a large range of reduced temperatures we had to add the regular background contribution found in Ref. [21], which is completely independent of the critical behavior described within our model.

Berg *et al.* did not only measure the real part of the shear viscosity but determined also the imaginary part of $\overline{\eta}$ from the phase shift. In Ref. [3] they compared the mode coupling result for the ratio $\mathrm{Im}(\overline{\eta})/\mathrm{Re}(\overline{\eta})$ with their experimental data and found good agreement. Comparing our results with these experimental data we get less satisfactory results [23] because in our theory the ratio $\mathrm{Im}(\overline{\eta})/\mathrm{Re}(\overline{\eta})$ approaches the finite value,

$$\lim_{T\to T_c}\frac{\mathrm{Im}(\overline{\eta})}{\mathrm{Re}(\overline{\eta})}=\frac{1}{76}\,\frac{\pi}{2}\left[1-\frac{1}{76}\{3\ln(1/4)-1/3\}\right]^{-1}\approx 0.0195, \tag{5.6}$$

at T_c which is different from the value 0.0353 obtained from the mode coupling theory with the exponent $x_\eta=0.069$ [3] which turns out to be in good agreement with the experimental data. As the limit of the ratio $\mathrm{Im}(\overline{\eta})/\mathrm{Re}(\overline{\eta})$ does not contain any free parameter at T_c it cannot be improved and the deviation of our theory from the experiments may be explained by the fact that a one-loop order perturbation theory is not able to describe such small effects (the imaginary part of the shear viscosity is only about 3% of the total complex shear viscosity) and therefore a two-loop theory may be expected to yield much better agreement. In this respect we should also note that the mode coupling expression used by Berg *et al.* is not purely of one-loop order since it makes use of the experimental value for the exponent x_η which differs significantly from its one-loop value. If we insert the one-loop value $x_\eta=1/19$ into the mode coupling expressions we would get a limit $\mathrm{Im}(\overline{\eta})/\mathrm{Re}(\overline{\eta})\approx 0.0271$ at T_c which is also significantly lower than the measured limiting ratio. So the main difference between the mode coupling theory and our theory is, that it is not possible to introduce the true critical exponent x_η in our expression for $\mathrm{Im}(\overline{\eta})/\mathrm{Re}(\overline{\eta})$ and therefore deviations from the one-loop order perturbation theory cannot be weakened by the use of the correct value for x_η.

VI. CONCLUSION

We were able to show that our one-loop perturbation theory result for the characteristic frequency evaluated within the field theoretical method of the renormalization group theory does not only reproduce the correct wave vector and correlation length dependence in the hydrodynamic region as well as in the critical region, but is also able to describe experimental data correctly for a large range of wave vectors and reduced temperatures. In addition we showed that also the result for the shear viscosity evaluated within the same model is in good agreement with experiments if a two-loop value for the critical exponent is taken.

There are however some points which indicate the need for a two-loop analysis of the model: First we have seen that in one-loop order the dynamic correlation function is always of Lorentzian form whereas scaling theory [8] predicts deviations for large frequencies. Second we are not able to get the experimental limiting value for the ratio of the imaginary and real part of the frequency dependent shear viscosity $\mathrm{Im}(\overline{\eta})/\mathrm{Re}(\overline{\eta})$ at T_c and we have to introduce a multiplicative factor for the frequency in order to describe the experimental data correctly. This makes a profound two-loop analysis inevitable which is currently in progress.

ACKNOWLEDGMENT

This work was supported by the Fonds zur Förderung der Wissenschaftlichen Forschung under Project No. P12422-TPH.

[1] P.C. Hohenberg, and B.I. Halperin, Rev. Mod. Phys. **46**, 435 (1977).
[2] R. Folk and G. Moser, Phys. Rev. E **57**, 683 (1998); **57**, 705 (1998).
[3] R.F. Berg, M.R. Moldover, and G.A. Zimmerli, Phys. Rev. Lett. **82**, 920 (1999); Phys. Rev. E **60**, 4079 (1999).
[4] G. Flossmann, R. Folk, and G. Moser, Phys. Rev. E **60**, 779 (1999).
[5] R. Folk and G. Moser, Phys. Rev. E **58**, 6246 (1998).
[6] P. Böni, H.A. Mook, J.L. Martinez, and G. Shirane, Phys. Rev. B **47**, 3171 (1992).
[7] H. Iro, Z. Phys. B: Condens. Matter **68**, 485 (1987); J. Magn. Magn. Mater. **73**, 175 (1988).
[8] R. Folk and G. Moser, in *Lectures on Cooperative Phenomena in Condensed Matter Physics*, edited by D. I. Uzunov (Heron, Sofia, 1996).
[9] Two-loop order calculations of the OP vertex functions lead to frequency dependent contributions and a non-Lorentzian shape function. However the consistency with its behavior for large frequencies remains an unsolved problem. G. Moser, R. Folk, and G. Flossmann (unpublished).
[10] R. Schloms and V. Dohm, Nucl. Phys. B **328**, 639 (1989); Phys. Rev. B **42**, 6142 (1990).
[11] J. Luettmer-Strathmann, J.V. Sengers, and G.A. Olchowy, J. Chem. Phys. **103**, 7482 (1995).
[12] K. Kawasaki and S.-M. Lo, Phys. Rev. Lett. **29**, 48 (1972).
[13] G. Paladin and L. Peliti, J. Phys. (France) Lett. **43**, 15 (1982), **45**, 289 (1984).
[14] H.C. Burstyn, J.V. Sengers, J.K. Bhattacharjee, and R.A. Ferell, Phys. Rev. A **28**, 1567 (1983)
[15] E.D. Siggia, B.I. Halperin, and P.C. Hohenberg, Phys. Rev. B **13**, 2110 (1976).
[16] H.L. Swinney and D.L. Henry, Phys. Rev. A **8**, 2586 (1973).
[17] R. Kita, K. Kubota, and T. Dobashi, Phys. Rev. E **58**, 793 (1998); **56**, 3213 (1997).
[18] G. Meier, B. Momper, and E.W. Fischer, J. Chem. Phys. **97**, 5884 (1992).
[19] The matching condition arises naturally in the calculation of the vertex function and we use in this way the freedom of choosing the flow parameter l in order to elliminate logarithmic terms.
[20] J.K. Bhattacharjee, R.A. Ferrell, R.S. Basu, and J.V. Sengers,

Phys. Rev. A **24**, 1469 (1981); J.K. Bhattacharjee and R.A. Ferrell, *ibid.* **27**, 1544 (1983).

[21] R.F. Berg and M.R. Moldover, J. Chem. Phys. **93**, 1926 (1990).

[22] The introduction of a multiplicative factor for the frequency alone is certainly no sufficient treatment of higher order effects but at least it changes the critical amplitude of the frequency dependence at T_c of the real part of the shear viscosity. In this way the critical limit ($\xi\rightarrow\infty$) of the theory is adjusted to experiment.

[23] R. Folk, Condens. Matter Phys. (to be published).